

FULLY PLASTIC FRACTURE MECHANICS FOR PLANE STRAIN CRACK GROWTH

F.A. McClintock, Y.J. Kim, and D.M. Parks
Massachusetts Institute of Technology
Cambridge, Massachusetts 02139, U.S.A.

ABSTRACT

A theoretical framework is given for designing possibly cracked structures to remain ductile under accidental overloads. For non-hardening, fully-plastic plane strain crack growth in a number of geometries and loadings, near tip fields are characterized by three parameters: the slip line angle θ , and the normal stress σ , and shear displacement δu , across the slip line. These parameters are found in terms of the far-field geometries and loadings through slip line fields or least upper bound analyses based on circular arcs. Then the crack growth criterion in terms of the crack tip opening angle (*CTOA*) is proposed as a function of near tip parameters and material properties. Experiments are suggested to determine the dependence of the *CTOA* on those variables.

INTRODUCTION

Under monotonic loading, structures should ideally be ductile, in order to provide both a warning before initial crack growth and continued resistance during crack growth. Such fully plastic behavior is of interest in design against collisions, tank car accidents, earthquakes, and ship groundings.

For brittle structures in tensile (Mode I) loading across a crack, only a criterion for initial growth is needed, because the crack is immediately unstable. The criterion is based on the discovery in the 1950's that there can be a region around the crack tip, large compared to either a plastic zone or to the microstructural fracture process zone, and small compared to the distance to the next nearest boundary, in which the stress and strain are uniquely defined in terms of a single parameter, the stress intensity factor K_I (see [1]). At a critical value for a given material, K_{IC} , the crack begins to grow unstably. (At lower values of K_I , the growth is negligible unless loading is repeated thousands of times as in fatigue.) The value of the applied K_I is determined from the far-field geometry and loading [2,3]. Thus for a brittle structure (one with a crack tip plastic zone small compared to any characteristic dimension of the part or to a crack in it), unstable crack growth occurs under the local condition

$$K_I(\text{geometry and loading}) \geq K_{IC}(\text{material}). \quad (1)$$

For more extensive plastic flow around a crack in a structure, it was found in the 1960's that for power-law strain hardening with $\sigma = \sigma_1 \epsilon^n$ and with a sufficiently high strain hardening exponent n , the stress and strain fields around a crack tip are characterized by another coefficient J , such that stable crack growth occurs under the local condition

$$J_I(\text{geometry, loading, } \sigma_1, n) \geq J_{IC}(\text{material}). \quad (2)$$

For crack growth large compared to the region in which a J -field dominates, the J -concept is no longer valid because it would have to be based on the current crack tip, and would not include the prior history which has left residual stresses and strain-hardening.

Asymptotic solutions have been found for an elastic-plastic growing crack, but the region in which the fracture strain dominates the yield strain turn out to be of sub-atomic size for the low strength alloys of interest here (see [4]).

For initial growth, the singular expansions giving the first-order coefficients K and J have been extended to higher stress levels (toward general yield) by including second-order coefficients T or Q [5,6], but the difficulties with finite crack growth remain.

For fully plastic flow in the limiting case of a vanishingly small strain hardening exponent n , the governing equations become hyperbolic, unique singular solutions do not exist, and the effects of far-field loading and geometry penetrate all the way to the crack tip in many cases [7]. For ductile alloys, elastic strains are negligible, and the fields of strain increments and stress for growing cracks are the same as for stationary cracks. The strain fields are then found by superposition of the strain increments for successive crack tip positions. Thus the known slip line fields for stationary cracks are applicable to growing cracks. The distortion of non-hardening fields by strain hardening is less in growing than in stationary cracks, because the advance of the fields through the material smooths out the discontinuities. Even in annealed aluminum, with a ratio of tensile to yield strength of 2.5, the deformation field around a growing crack (shear bands around a rigid wedge in front of the crack) shows a strong resemblance to the non-hardening field (see [8], p. 378).

Here we review the extension of fracture mechanics to the limiting case of non-hardening, plane strain crack growth. It turns out that for Mode I loading, many of the infinite variety of non-hardening stress and strain fields can be usefully approximated by just three parameters. (For unsymmetrical fields, see [9].) While three parameters are more than for brittle structures or for the ductile initiation of crack growth discussed above, this theory should provide a guide for the design of crack-resistant structures of common low-strength alloys.

NEAR-TIP FIELD CHARACTERIZATION FROM SLIP LINE FIELD ANALYSIS

Fields of stress and displacement increments for cracked structures of rigid-plastic, non-hardening materials have been found for a variety of geometries and loadings (see [7,10]). At the crack tip, a number of these fields consist simply of a pair of slip lines surrounded by rigid regions, e.g., the single-face-cracked specimens under bending (Fig. 1a). Other fields consist of a pair of deforming fans surrounded by regions with less concentrated plastic flow, e.g., the doubly grooved specimens under tension (Fig. 1b). To simplify the problem, regard the deformation in the fan at the crack tip as being concentrated on a single slip line which is surrounded by rigid regions.

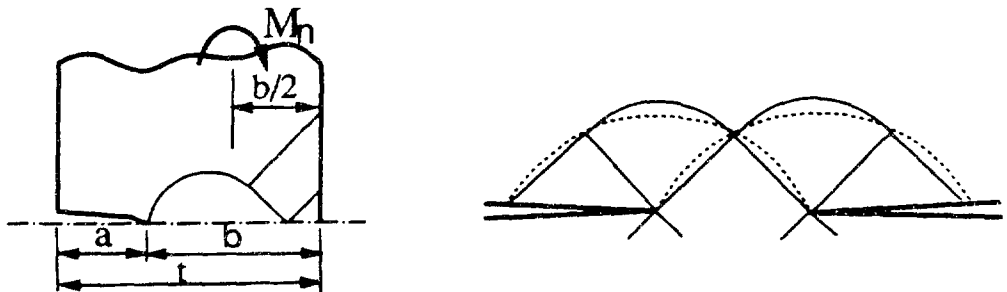


Fig. 1. Slip line fields (a) for a deep, single-face-cracked plate under pure bending, and (b) a symmetric doubly-cracked plate in tension.

For symmetric geometry and loading, the near tip fields are now characterized by just three parameters: the slip line angle θ , and the normal stress σ , and shear displacement δu , across the slip line. This three-parameter characterization of near tip fields in fully plastic fracture crack

growth mechanics presents a contrast to the one-parameter (K) in elastic fracture mechanics or the two-parameter (K or J and T or Q) characterization in linear or non-linear elastic fracture mechanics.

If pairs of slip lines are available for the problem at the hand, they describe a local field. (as does K) as a function of loading and geometry:

$$\left\{ \begin{array}{l} \theta_s \\ \sigma_s \\ \delta u_s \end{array} \right\} = \{ f \} \text{ (far-field geometry, loadings, and their increments).} \quad (3)$$

Now consider forms of (3) for cases in which the slip line fields are not available or are more complicated than pair of slip lines.

NEAR-TIP FIELD CHARACTERIZATION FROM LEAST UPPER BOUND ANALYSIS

Finding θ_s and δu_s

The least upper bound (LUB) field with a circular arc provides an estimate not only of the limit load, but also of the slip plane angle θ , and displacement δu_s , all in terms of far-field geometry and loadings. For example, consider a single-face-cracked plate with shear strength k , subject to combined bending and large tension (Fig. 2a). For given net section shear $V_n (= 0)$ and tension N_n , the LUB to the moment M_n can be found by minimizing M_n determined from relative sliding along the circular arc with respect to two independent arc parameters, α and β . The yield locus from the LUB analysis is shown in Fig. 2b, including that where slip line fields are known [11]. Figure 2b also includes results from finite element limit analysis by Lee and Parks [12]. For predominant bending ($0 \leq N_n/(2kb) < 0.55$), FEM results are consistent with the SLF solutions. For combined bending with large tension ($0.55 \leq N_n/(2kb) \leq 1.0$), the locus from the LUB analysis is no more than 3% above the FEM results.

The LUB field also provides δu_s , (or the crack tip opening displacement increment $\delta CTOD$) in terms of far field increments of displacement δu and rotation $\delta\theta$ (Fig. 2a):

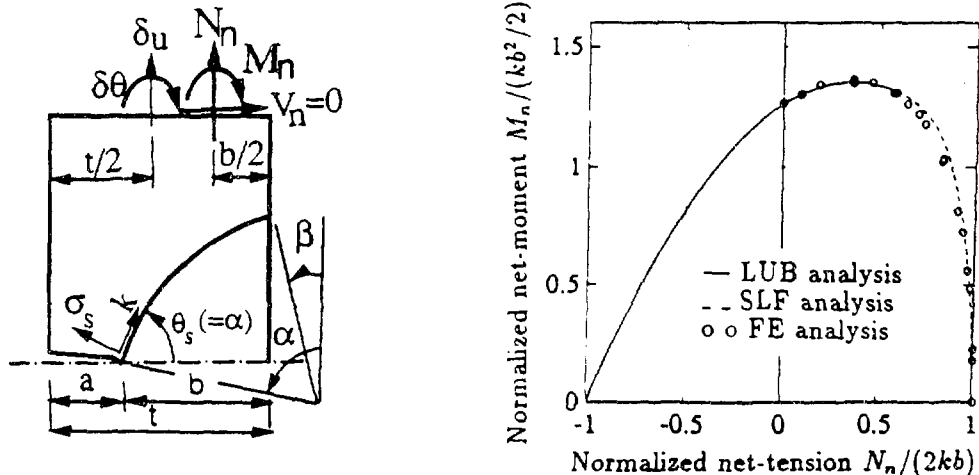


Fig. 2. (a) Circular arc for an upper bound in a deep, single-face-cracked specimen under combined bending and large tension, and (b) limit loads from the least upper bound field and FEM results.

$$\delta u_s \left(= \frac{\delta CTOD/2}{\sin \theta_s} \right) = \frac{1}{\sin \theta_s} \left[\delta u + \left(\frac{t}{2} - a \right) \delta \theta \right]. \quad (4)$$

Finding σ_s

It is very difficult to glean information on the local stress from lower bound stress fields satisfying equilibrium, the yield condition, and traction boundary conditions. We show here a new method of approximating σ_s from the least upper bound.

Consider rigid-body rotation across a circular arc extending from a crack tip across a ligament of width b in a plate with shear strength k (Fig. 3), subject to general loading with three components: V , N , and M . Suppose that two loading components are specified and that the circular arc for the LUB to the unspecified loading component has been found. Along the arc, the shear component of traction is k . Then the following theorem holds, as proven in [13].

Assume that the normal component of traction, σ , on the LUB arc satisfies the first Hencky equation of equilibrium with one unknown (the reference stress σ_r) evaluated at $\psi = 0$:

$$d\sigma = 2kd\psi \quad \text{or} \quad \sigma = \sigma_r + 2k\psi. \quad (5)$$

Then if σ_r is chosen to satisfy force equilibrium in any other than the chordal direction (the 1-direction in Fig. 3), the tractions on the LUB arc satisfy global equilibrium.

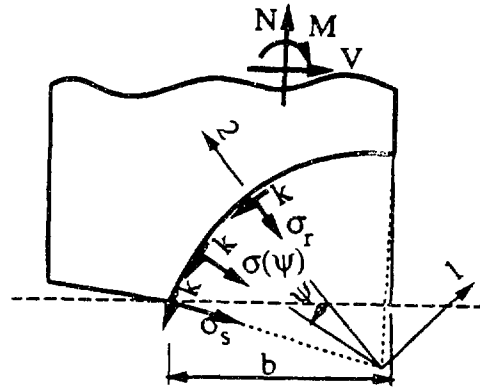


Fig. 3. Kinematically admissible plane strain deformation field consisting of rigid-body rotation across a circular arc in a cracked plate.

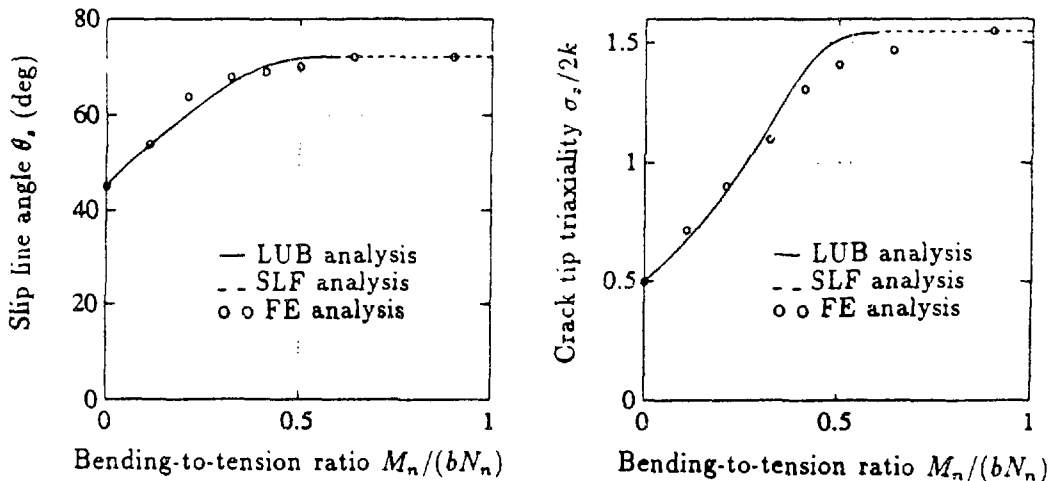


Fig. 4. Near tip slip angle θ_s and crack tip stress triaxiality $\sigma_s/(2k)$ for deep, single-face-cracked plates under combined bending and tension.

The normal stress across the LUB arc at the crack tip, σ_s , can be approximated from the Hencky equation (5) with the determined reference stress σ_r . Therefore the LUB arc provides an approximation to the stress and deformation fields at a crack tip, consistent with global equilibrium.

To test accuracy with an example, consider again the single-face-cracked plate under combined bending and large tension (Fig. 2a), for which exact slip line field solutions are not known but finite element results are available [12]. (As shown in Fig. 4 for various bending-to-tension ratios, at the ends of the curves where SLF results are available, θ_s and $\sigma_s/2k$ are consistent with the SLF values, except that $\sigma_s/2k$ is 5% low at $M_n/(bN_n) = 0.64$.) For bending with large tension, the LUB values of θ_s and $\sigma_s/2k$ appear accurate within 5%. The accuracy of the third parameter, δu_s , is not available from the FEM results, but for pure tension and for the modified Green and Hundy field with $M_n/(bN_n) = 0.60$, δu_s from the LUB is exactly that from the SLF. (This agreement is somewhat coincidental, because for pure bending δu_s from the LUB is 1.4 times that from the SLF.)

The accuracy of the LUB analysis has also been considered for three cases with known SLF [13]. For a single-face-cracked plate in pure shear, θ_s from the LUB analysis is zero compared to $\pm 8.2^\circ$ from the SLF analysis; $\sigma_s/2k$ is zero compared to ± 0.14 , and δu_s is exact. For a three-point bend plate with a total length to ligament ratio of 6, θ_s from the LUB analysis is 56° compared to 68° ; $\sigma_s/2k$ is 1.06 compared to 1.22, and δu_s is 2.4 times the SLF value for the same end displacements. As here, the agreement is worst with fields involving constant state regions or fans. For the classical double-face-cracked plate in tension, the fan runs from 45° to 135° with $\sigma_s/2k$ falling from 2.1 to 0.5; θ_s from the LUB analysis comes in at a reasonable $\theta_s = 68^\circ$, but $\sigma_s/2k$ is high at 2.54, δu_s is low by a factor of 0.5 to 0.67, depending on whether the Prandtl, Hill, or Neimark displacement field is used for comparison. In this case, improved agreement would require more parameters in the fracture criterion. In other cases, values from the LUB analysis might be improved by extend the LUB fields to include constant deformation fields, as well as arcs.

CRACK GROWTH CRITERION

With the local field characterized by θ_s , σ_s , and δu_s , we turn to the response of the material by crack growth δa in terms of those parameters. The response can be expressed in terms of the crack tip opening angle *CTOA*:

$$\delta a(\theta_s, \sigma_s, \delta u_s) = \frac{\delta u_s \sin \theta_s}{\tan(CTOA/2)}, \text{ where } CTOA(\theta_s, \sigma_s, \text{material}). \quad (6)$$

The functional form of *CTOA* should ultimately be determined by experiment, just as is K_{IC} . Such experiments are outlined below, but for insight, first consider a micromechanical model.

A sliding off and shear-cracking model for a growing crack

Consider zig-zag crack growth, sliding off by s and cracking by c along a shear band before changing direction (Fig. 5). The geometry gives the form of *CTOA* in terms of θ_s and s/c :

$$\tan\left(\frac{CTOA}{2}\right) = \frac{s \sin \theta_s}{(c + c + s) \cos \theta_s} = \frac{1}{2(c/s) + 1} \tan \theta_s. \quad (7)$$

Geometry also gives the relation between the fracture shear strain in the band γ_f , and s and c :

$$\gamma_f = \frac{s}{(s + c) \sin 2\theta_s}. \quad (8)$$

Eliminating (c/s) in (7) with (8) gives

$$\tan\left(\frac{CTOA}{2}\right) = \frac{1}{[2/(\gamma_f \sin 2\theta_s) - 1]} \tan \theta_s. \quad (9)$$

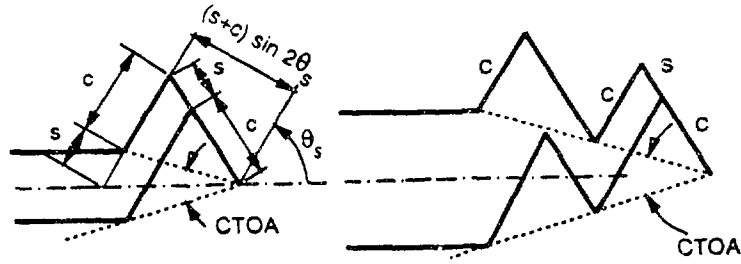


Fig. 5. Sliding off and shear cracking model for a growing crack.

Equation (9) gives the $CTOA$ in terms of θ_s and γ_f . The fracture strain γ_f will depend on the mean normal stress in the shear band, σ_s , and on material properties such as hardening and an initial volume fraction of holes, which will be discussed next.

Fracture strain in the shear band

Accounting for micromechanisms for crack growth such as hole nucleation, hole growth, and linkage by localization or fine cracking, McClintock et al. [4] proposed

$$\gamma_f = \frac{(1-n)A}{\sinh[(1-n)\sigma_s/k]} + B(\sigma_s), \quad (10)$$

where A and B are parameters and n is the strain hardening exponent in $k = k_0 \gamma^n$ with $k_0 = \text{constant}$. The first term on the RHS of (10) can be viewed as a strain for hole growth to linkage by localization or by fine cracking [14]. The second term, $B(\sigma_s)$, can be viewed as a strain for hole nucleation, which is generally a function of mean normal stress [15]. For preliminary insight, assume the nucleation strain is negligible ($B = 0$). Figure 6a shows an inverse exponential dependence on σ_s/k for non-hardening ($n = 0$) flow and for typical values of A , ranging from 0.2 to 1.2, along with limited available experimental data on $CTOA$ from the literature [16,17]. Hancock et al. [18] performed fully plastic (crack initiation and growth) tests providing a wide range of crack tip triaxiality: three point bending, compact tension, and center cracked panel (CCP) test. (Their CCP test specimens did not meet plane strain requirements, so the resulting crack tip triaxiality would be lower than that for single-face-cracked specimens in tension.) Their results also showed a dramatic decrease in $CTOA$ with increasing σ_s/k as in Fig. 6a. Figure 6b shows a higher order parabolic dependence on θ_s ($45^\circ \leq \theta_s \leq 72^\circ$) for non-hardening ($n = 0$) and for two values of $A = 1.0, 0.5$. Therefore, to a first order for small n , (9) with (10) suggests that the $CTOA$ has inverse exponential dependence

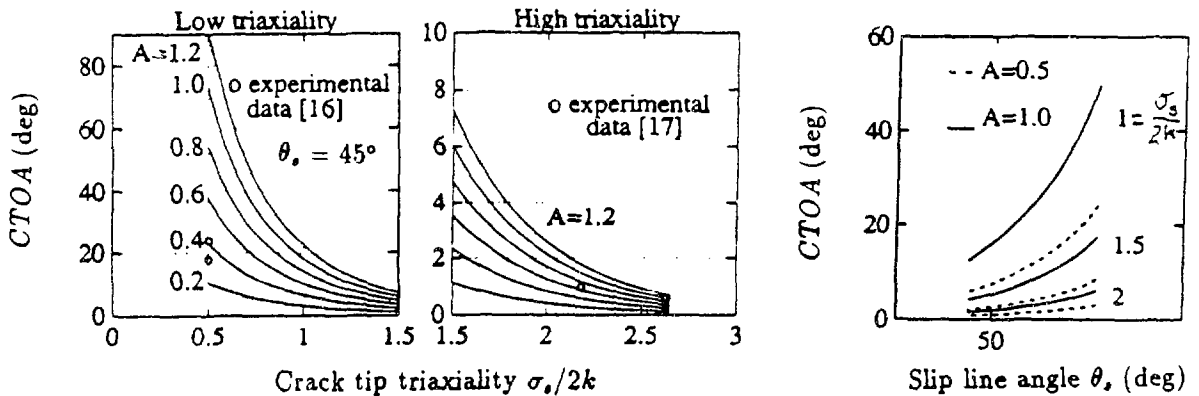


Fig. 6. Dependence of the estimated crack tip opening angle ($CTOA$) on $\sigma_s/(2k)$ and θ_s . Equation (9) and (10) with $n = 0$ and $B = 0$.

on σ_s/k and higher order parabolic dependence on θ_s for $45^\circ \leq \theta_s \leq 72^\circ$.

Note that (10) is analogous to K_{IC} (material), and therefore the parameters A and B in (10) reflect material properties and should be found from fully plastic crack growth experiments, as follows.

Suggested experimental determination of CTOA

The functional dependence of $CTOA(\theta_s, \sigma_s)$, on the parameters A and B of the fracture criterion of (9) with (10), can be found by fully plastic crack growth tests. For example, at $\theta_s = 45^\circ$, $\sigma_s/2k$ can be increased from 0.5 to 1.547 in the unequally grooved specimens of Fig. 7a by decreasing the back-angle 2ϕ from 180° to 60° [7]. Solving (9) with (10) from the experimental data would allow fitting the constants A and B . For higher values of θ_s , consider the 4-point bending specimen of Fig. 7b. According to the SLF analysis [19], decreasing the back-angle 2ϕ from 180° to 90° would increase $\sigma_s/2k$ from 1.177 to 1.543 with θ_s nearly constant in the range from 67° to 72° . The constants A and B found from fitting these data should be the same as those from the unequally grooved tensile tests.

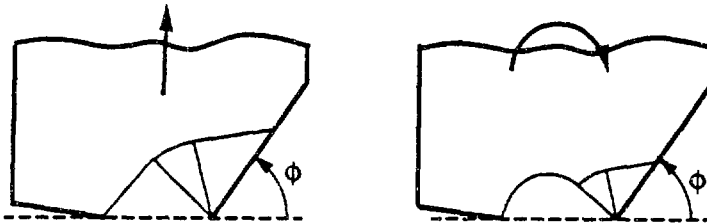


Fig. 7. Slip line fields for unequally grooved specimens (a) under pure extension, and (b) under pure bending.

CONCLUSION

For designing possibly cracked structures that must remain ductile under accidental overloads, we present a practical theory for fully plastic, plane strain crack growth. The one or two parameter characterization in linear or nonlinear elastic fracture mechanics must be extended to three parameters for the near tip fields of a growing crack in fully plastic, plane strain conditions: the slip line angle θ_s , and the normal stress σ_s , and shear displacement δu_s , across the slip line. These parameters are found for the geometry and loading condition either from slip line field analysis or from least upper bound analysis based on a circular arc using only a programmable calculator. This is analogous, for example, to the K_I (geometry and loadings) of linear elastic fracture mechanics.

The material function analogous to K_{IC} (material) is expressed as the dependence of the crack tip opening angle (CTOA) on σ_s , θ_s , and material properties. This dependence should be determined from fully plastic crack growth tests, which are suggested.

ACKNOWLEDGEMENT

This work was supported by the Office of Basic Energy Sciences, Department of Energy, under Grant DE-FG02-85ER13331 to M.I.T. and Contract DE-AS07-761D01670 with the Idaho National Energy Laboratory.

REFERENCES

1. M.F. Kanninen and C.H. Popelar, *Advanced Fracture Mechanics*, Oxford University Press, New York (1985).

2. H. Tada, P.C. Paris and G.R. Irwin, *The Stress Analysis of Cracks Handbook*, Paris Productions Inc., Saint Louis, MO (1985).
3. Y. Murakami, *Stress Intensity Factors Handbook*, Pergamon Press, Oxford (1987).
4. F.A. McClintock, Y.J. Kim and D.M. Parks, "Criteria for Fully Plastic, Plane Strain Crack Growth", *Int. J. Fracture* (submitted for publication).
5. D.M. Parks, "Advances in Characterization of Elastic-Plastic Crack-Tip Fields", in *Topics in Fracture and Fatigue*, Springer-Verlag, 59 (1991).
6. N.P. O'Dowd and C.F. Shih, "Family of Crack-Tip Fields Characterized by A Triaxiality Parameters - II. Fracture Application", *J. Mech. Phys. Solids* 40, 939 (1992).
7. F.A. McClintock, "Plasticity Aspects of Fracture", in *Fracture Vol. 3*, Academic Press, New York 47 (1971).
8. F.A. McClintock and A.S. Argon, *Mechanical Behavior of Materials*, Addison Wesley (1966).
9. F.A. McClintock, "Reduced Crack Growth Ductility Due to Asymmetric Configurations", *Int. J. Fracture* 42, 357 (1990).
10. B.B. Hundy, "Plane Plasticity", *Metallurgia* 49, 109 (1956).
11. M. Shiratori and B. Dodd, "Effect of Deep Wedge-Shaped Notches of Small Flank Angle on Plastic Failure," *Int. J. Mech. Sci.* 22 127, (1980).
12. H. Lee and D.M. Parks, "Fully Plastic Analyses of Plane Strain Single Edge Cracked Specimens Subject to Combined Tension And Bending", *Int. J. Fracture* (submitted for publication).
13. Y.J. Kim, F.A. McClintock and D.M. Parks, "Global Equilibrium of the Least Upper Bound Circular Arcs and its Application to Fracture Mechanics", *J. Mech. Phys. Solids* (submitted for publication).
14. F.A. McClintock, S.M. Kaplan and C.A. Berg, "Ductile Fracture by Hole Growth in Shear Bands", *Int. J. Fract. Mech.* 17, 201 (1966).
15. A.S. Argon, J. Im and R. Safoglu, "Distributuion of Plastic Strain and Negative Pressure in Necked Steel and Copper Bars", *Metallurgical Transcations*, 6A 815 (1975).
16. G.A. Kardomateas and F.A. McClintock, "Shear Band Characterization of Mixed Mode I and II Fully Plastic Fracture", *Int. J. Fracture* 40, 1 (1989).
17. F.A. McClintock and S.J. Wineman, "A Wedge Test for Quantifying Fully Plastic Fracture", *Int. J. Fracture* 33, 285 (1987).
18. J.W. Hancock, W.G. Reuter and D.M. Parks, "Constraint and Toughness Parameterized by T^* ", to appear in *ASTM STP on Constraint Effects in Fracture, Proc. ASTM Symposium*, Indianapolis, IN (1991).
19. Y.J. Kim, "Modeling Fully Plastic Plane Strain Crack Growth", Ph.D. Thesis, Department of Mechanical Engineering, MIT, Cambridge, MA (in progress).